Two-dimensional surface emitting photonic crystal laser with hybrid triangular-graphite structure

Luis Javier Martínez[1,*], Benito Alén[1], Ivan Prieto[1] , J.F. Galisteo-López[2], Matteo Galli[2], Lucio Claudio Andreani[2], Christian Seassal[3], Pierre Viktorovitch[3], and Pablo Aitor Postigo[1]

[1]*Instituto de Microelectrónica de Madrid (CNM, CSIC), Isaac Newton 8, E-28760, Tres Cantos Madrid, Spain*

[2]*Dipartimento di Fisica "A. Volta" and UdR CNISM, Università degli Studi di Pavia, via Bassi 6, I-27100 Pavia, Italy*

[3]*Université de Lyon, Institut des Nanotechnologies de Lyon-INL, UMR CNRS 5270, Ecole Centrale de Lyon, 36 Avenue Guy de Collongue, F-69134 Ecully, France*

[*]*Corresponding author: luisja@imm.cnm.csic.es*

Abstract: We present laser emission of a compact surface-emitting micro laser, optical pumped and operating at 1.5 μm at room temperature. A two-dimensional photonic crystal lattice conformed in a hybrid triangular-graphite configuration is designed for vertical emission. The structures have been fabricated in an InP slab, including four InAsP quantum wells as active layer, on the top of a Si substrate SiO_2 wafer bonded. Laser emission with thresholds around 70 μW and quality factors (Qs) up to 12000 have been measured. The Bloch mode selected for the emission keeps a high Q ($\geq 2\times10^5$) around the Γ point for a wide range of in-plane values $k_{||} \leq 0.1(2\pi/a)$ which is related to peculiar properties of the hybrid lattice.

OCIS codes: (160.5298) Photonic crystals; (130.0250) Optoelectronics; (250.5300) Photonic integrated circuits

References and links

1. E. Yablonovitch, "Inhibited spontaneous emission in solid-state physics and electronics," Phys. Rev. Lett. **58**, 2059-2062 (1987).
2. S. John, "Strong localization of photons in certain disordered dielectric superlattices," Phys. Rev. Lett. **58**, 2486-2489 (1987).
3. O. Painter, R.K. Lee, A. Scherer, A. Yariv, J.D. O'Brien, P.D. Dapkus, I. Kim, "Two-Dimensional Photonic Band-Gap Defect Mode Laser," Science, **284**, 1819-1821, (1999).
4. S-H Kim, H-Y Ryu, H-G Park, G-H Kim, Y-S Choi, Y-H Lee, and J-S Kim, "Two-dimensional photonic crystal hexagonal waveguide ring laser," Appl. Phys. Lett. **81**, 2499-2501 (2002).
5. A. R. Alija, L. J. Martínez, P. A. Postigo, C. Seassal, and P. Viktorovitch, "Coupled-cavity two-dimensional photonic crystal waveguide ring laser," Appl. Phys. Lett. **89**, 101102 (2006).
6. X. Letartre, C. Monat, C. Seassal, and P. Viktorovitch, "Analytical modeling and an experimental investigation of two-dimensional photonic crystal microlasers: defect state (microcavity) versus band-edge state (distributed feedback) structures," J. Opt. Soc. Am. B **22**, 2581-2595 (2005).
7. S. Boutami, B. Ben. Bakir, L-L Leclercq, X. Letartre, Ch. Seassal, P. Rojo-Romero, P. Regreny, M. Garriges, and P. Viktorovitch, "Photonic Crystal-Based MOEMS Devices," IEEE J. Quantum Electron. **13**, 244-252 (2007).
8. S. Strauf, K. Hennessy, M. T. Rakher, Y.-S. Choi, A. Badolato, L. C. Andreani, E. L. Hu, P. M. Petroff, and D. Bouwmeester, "Self-Tuned Quantum Dot Gain in Photonic Crystal Lasers," Phys. Rev. Lett. **96**, 127404 (2006).
9. C. Monat, C. Seassal, X. Letartre, P. Regreny, P. Rojo-Romeo, P. Viktorovitch, M. Le Vassor d'Yerville, D. Cassagne, J. P. Albert, E. Jalaguier, S. Pocas, and B. Aspar, "InP based 2-D photonic crystal on silicon: In-plane Bloch mode laser," Appl. Phys. Lett. **81**, 5102-5104 (2002).

#112644 - $15.00 USD Received 10 Jun 2009; revised 18 Jul 2009; accepted 20 Jul 2009; published 10 Aug 2009

10. S-H Kwon, H-Y Ryu, G-H Kim, Y-H Lee, and S-B Kim, "Photonic bandedge lasers in two-dimensional square-lattice photonic crystal slabs," Appl. Phys. Lett. **83**, 3870-3872 (2003).
11. H-Y Ryu, S-H Kwon, Y-J Lee, Y-H Lee, and J-S Kim, "Very-low-threshold photonic band-edge lasers from free-standing triangular photonic crystal slabs," Appl. Phys. Lett. **80**, 3476-3478 (2002).
12. J. Mouette, C. Seassal, X. Letartre, P. Rojo-Romeo, J. L. Leclercq, P. Regreny, P. Viktorovitch, E. Jalaguier, P. Perreau, and H. Moriceau, "Very low threshold vertical emitting laser operation in InP graphite photonic crystal slab on silicon," Electron. Lett. **39**, 526-528 (2003).
13. Y. Park, S. Kim, Ch. Moon, H. Jeon, and H. Jin Kim, "Butt-end fiber coupling to a surface-emitting Γ-point photonic crystal band edge laser," Appl. Phys. Lett. **90**, 171115 (2007).
14. L.J. Martínez, A. García-Martín, and P. Postigo, "Photonic band gaps in a two-dimensional hybrid triangular-graphite lattice," Opt. Express **12**, 5684-5689 (2004).
15. A.R. Alija, L.J. Marínez, P.A. Postigo, J. Sánchez-Dehesa, M. Galli, A. Politi, M. Patrini, L.C. Andreani, C. Seassal, and P. Viktorovitch, "Theoretical and experimental study of the Suzuki-phase photonic crystal lattice by angle-resolved photoluminescence spectroscopy," Opt. Express **15**, 704-713 (2007).
16. S. David, A. Chelnokov, and J.-M. Lourtioz, "Isotropic Photonic Structures: Archimedean-Like Tilings and Quasi-Crystals," IEEE J. Quantum Electron. **37**, 1427-1434 (2001).
17. H. Altug and J. Vučković, "Two-dimensional coupled photonic crystal resonator arrays," Appl. Phys. Lett. **84**, 161-163 (2004).
18. L. C. Andreani and D. Gerace, "Photonic-crystal slabs with a triangular lattice of triangular holes investigated using a guided-mode expansion method," Phys. Rev. B , **73**, 235114 (2006).
19. L. J. Martínez, A. R. Alija, P. A. Postigo, J. F. Galisteo-López, M. Galli, L. C. Andreani, Ch. Seassal, and P. Viktorovitch, "Effect of implementation of a Bragg reflector in the photonic band structure of the Suzuki-phase photonic crystal lattice," Opt. Express **16**, 8509-8518 (2008).
20. B.S. Song, S. Noda, T. Asano, and Y. Akahane, "Ultra-high-Q photonic double-heterostructure nanocavity," Nature Materials **4**, 207-210 (2005).
21. C. Seassal, C. Monat, J. Mouette, E. Touraille, B. Ben Bakir, H. T. Hattori, J. L. Leclercq, X. Letartre, P. Rojo-Romeo, and P. Viktorovitch, "InP bonded membrane photonics components and circuits: toward 2.5 dimensional micro-nano-photonics," IEEE J. Quantum Electron. 11, 395-407 (2005).
22. L. J. Martínez, I. Prieto, B. Alén, and P. A. Postigo, "Fabrication of high quality factor photonic crystal micro-cavities in InAsP/InP membranes combining reactive ion beam etching and reactive ion etching," J. Vac. Tech. B **27**, 1801-1804 (2009).
23. T. Baba and D. Sano, "Low-threshold lasing and Purcell effect in microdisk lasers at room temperature," IEEE J. Quantum Electron. **10**, 1340-1346 (2003).
24. E. D. Palik, Handbook of Optical Constants of Solids, (Academic Press, INC., Orlando, Florida, USA, 1985).
25. K. Srinivasan, P.E. Barclay, O. Painter, J. Chen, A.Y. Cho, C. Gmachl, "Experimental demonstration of a high-Q photonic crystal microcavity," Appl. Phys. Lett. , **83**, 1915-1917 (2003).
26. C. Wilmsen, H. Temkin, and L. A. Coldren, Vertical-Cavity Surface-Emitting Lasers, (Cambridge University Press, Cambridge UK, 1999).
27. C. Monat, C. Seassal, X. Letartre, P. Regreny, P. Rojo-Romeo, P. Viktorovitch, M. Le Vassor d'Yerville, D. Cassagne, J.P. Albert, E. Jalaguier, S. Pocas, and B. Aspar, "Modal analysis and engineering of InP-based two-dimensional photonic crystal microlasers on a silicon wafer," IEEE J. Quantum Electron. **39**, 419-425 (2003).
28. D. Kuksenkov, S. Feld, C. Wilmsen, H. Temkin, S. Swirhun, and R. Leibenguth,"Linewidth and alpha-factor in AlGaAs/GaAs vertical cavity surface emitting lasers," Appl. Phys. Lett. ,**66**, 277-279 (1995).
29. B. Ben Bakir, C. Seassal, X. Letartre, P. Regreny, M. Gendry, P. Viktorovitch, M. Zussy, L. Di Cioccio, and J.-M. Fedeli, "Room-temperature InAs/InP Quantum Dots laser operation based on heterogeneous "2.5 D" Photonic Crystal," Opt. Express **14**, 9269-9276 (2006).
30. F. Raineri, C. Cojocaru, R. Raj, P. Monnier, A. Levenson, C. Seassal, X. Letartre, and P. Viktorovitch, "Tuning of a two-dimensional photonic crystal resonance via optical carrier injection," Opt. Lett. **30**, 64-66 (2005).
31. L. Ferrier, O. El Daif, X. Letartre, P. Rojo-Romeo, Ch. Seassal, R. Mazurczyk, and P. Viktorovitch, "Surface emitting microlaser based on 2D photonic crystal rod lattices," Opt. Express **17**, 9780-9788 (2009).
32. L. Ferrier, P. Rojo-Romero, E. Drouard, X. Letartre, and P. Viktorovitch, "Slow Bloch mode confinement in 2D photonic crystals for surface operating devices," Opt. Express **16**, 3136-3145 (2008).
33. F. Bordas, M. J. Steel, Ch. Seassal, and A. Rahmani, "Confinement of band-edge modes in a photonic crystal slab," Opt. Express **15**, 10890-10902 (2007).
34. F. Bordas, Ch. Seassal, E. Dupuy, Ph. Regreny, M. Gendry, P. Viktorovitch, M. J. Steel, and A. Rahmani, "Room temperature low-threshold InAs/InP quantum dot single mode photonic crystal microlasers at 1.5 μm using cavity-confined slow light," Opt. Express **17**, 5439-5445 (2009).

#112644 - $15.00 USD Received 10 Jun 2009; revised 18 Jul 2009; accepted 20 Jul 2009; published 10 Aug 2009

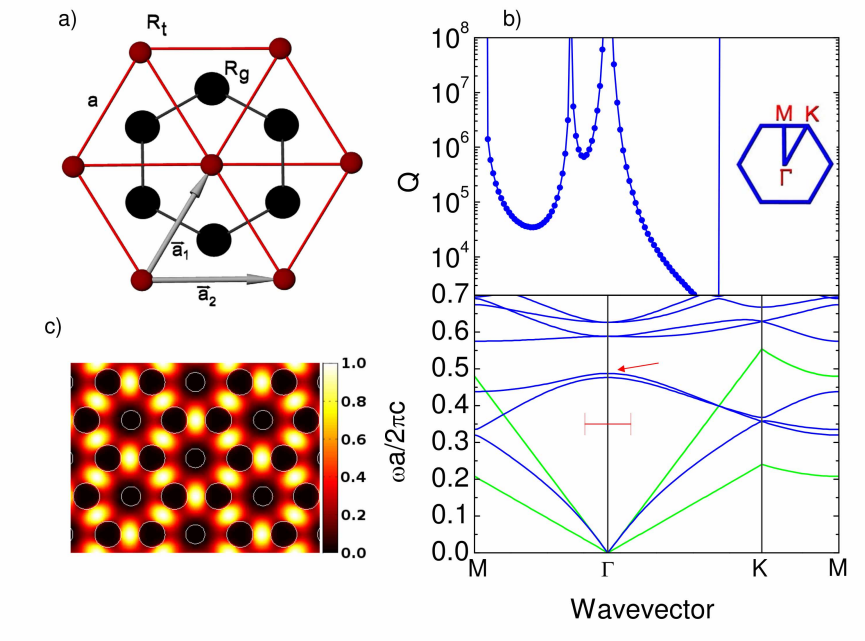

Fig. 1. a) Schematic representation of the hybrid triangular-graphite lattice and the high symmetry directions in the k space. b) Calculated quality factor of the third band and photonic band structure (only even modes $\hat{\sigma}_{xy} = +1$ are plotted). Upper green line represents the light line with the average cladding dielectric constant. Bottom green line represents the InP light line. The red bar denotes the region with $k_{||}$ <0.1(2π/a) around the Γ point, where the Γ_3 band (indicated by a red arrow) is flat. c) Normalized E-field intensity profile at the Γ_3 point. The parameters of the gme simulation are: $a = 780$ nm, $R_t/a = 0.12$, $R_g/a = 0.17$, $\varepsilon = 10.1$, $t/a = 0.304$.

1. Introduction

Since the proposal that certain periodic dielectric structures present a photonic band gap and this could inhibit the spontaneous emission [1, 2] even in two dimensions (2D), they have been used to control the light in the wavelength scale especially to fabricate low-threshold lasers. Several kinds of 2D-slab photonic crystal (PC) lasers have been studied up to now. Microcavity PC lasers [3], ring-like lasers [4, 5], large area PC lasers [6], and recently the so-called 2.5-D microresonators [7] are some of the examples. In microcavity lasers a high quality factor (Q) and small modal volume are necessary in order to get low threshold emission [8]. Other 2D-slab PC lasers are based in the low group velocity close to the high symmetry points of the reciprocal lattice [9, 10, 11, 12]. In this way the light-matter interaction is increased and laser operation is reached easier. One part of those band-edge PC lasers use specific reciprocal points below the light line [9, 10]. In that case the light is confined in the vertical direction by total internal reflexion (TIR) and the optical losses are mainly in-plane due to the finite size of the structure. The other part is based in the low dispersive bands close to the Γ point [11, 12]. In that case, if the Bloch modes are weakly coupled to the radiative modes laser emission can be reached. The emission is very directional around the Γ point favoring the efficient coupling to, for example, an optical fiber [13]. The threshold and Q vary widely among those structures depending on the kind of the PC lattice, its size and the active material used. In this paper we demonstrate laser emission at 1.55 μm in a Γ-point PC laser conformed in the hybrid triangular-graphite lattice

#112644 - $15.00 USD Received 10 Jun 2009; revised 18 Jul 2009; accepted 20 Jul 2009; published 10 Aug 2009

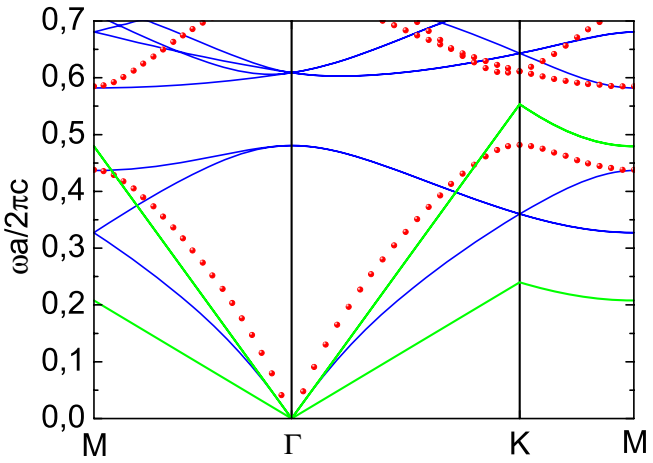

Fig. 2. Photonic band structures (only even modes $\hat{\sigma}_{xy} = +1$ are plotted) of the triangular lattice calculated with the same filling factor that the hybrid lattice of Fig. 1 (b). The parameters of the gme simulation are: $a = 780$ nm, $R_t/a = 0.155$, $R_g/a = 0.155$, $\varepsilon = 10.1$, $t/a = 0.304$. Blue line: calculated with the Bravais lattice of the hybrid triangular-graphite. Red dots: calculated with its natural Bravais lattice ($a \longrightarrow a/\sqrt{3}$). Green lines are the light lines of the average cladding and core materials.

[14] with low-threshold and a high Q. Specifically, we have used the Γ_3 point of the photonic bands due to its special properties: first, it favours the vertical emission. Second, the Bloch mode selected presents a large vertical quality factor $Q_v \geq 2 \times 10^5$, and third, this happens for a wide set of in-plane values $k_{||} \leq 0.1(2\pi/a)$ (see vertical red bars in Fig.1(b)). This high Q for a large set of $k_{||}$ values above the light line is because the selected Bloch mode at Γ_3 of the hybrid lattice (see red arrow in Fig. 1 (b)) corresponds also to the maximum of the first K_1 point of the triangular lattice, which is below the light line. That point becomes weakly radiative by the small perturbation corresponding to the different radius between the two set of holes of the hybrid lattice, as we discuss in the paper.

2. Design

The hybrid triangular-graphite lattice was created as a perturbation of the triangular lattice where a reduction of the radii of some of the holes of the triangular lattice (with lattice constant $a/\sqrt{3}$) gives birth to a new hybrid structure where two sublattices with triangular and graphite symmetries (that share the same Bravais lattice with underlying lattice constant a, (see Fig. 1 (a)). This hybrid triangular-graphite lattice belongs to a set of 2D structures, like the Suzuki-phase [15] and the Archimedean [16] lattices, which have a basis made of several rods per unit cell, similar to coupled cavity arrays [17]. All these lattices seem to support several low-dispersive photonic bands. Figure 1 (b) shows the band structure of the hybrid triangular-graphite lattice and the Q calculated for the third band (TE-like mode) using the guided-mode expansion method (gme) in the symmetric approach [18, 15]. This approach has shown a good agreement between the calculated band structure of 2D PC waveguides embedded in air and SiO_2 [15, 19] and the measured ones. We have selected the Γ_3 point of the third band for the

#112644 - $15.00 USD Received 10 Jun 2009; revised 18 Jul 2009; accepted 20 Jul 2009; published 10 Aug 2009

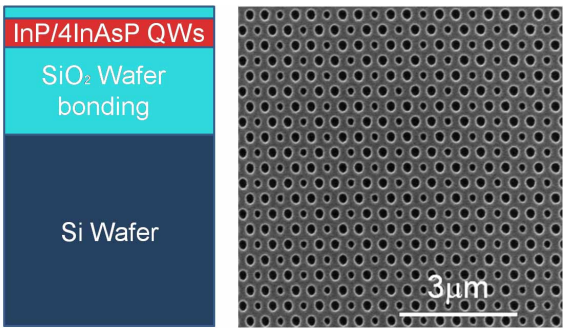

Fig. 3. a) Layout of the transversal section of the fabricated structures. b) Scanning electron microscopy image of a fabricated structure. The lattice parameter is $a \simeq 780$ nm, $R_t/a \sim 0.12$ and $R_g/a \sim 0.17$.

laser emission. At this point the photonic band structure presents a well isolated hexapole Bloch mode (Fig. 1 (c)) with low dispersion and negative curvature around the Γ_3 point. This mode is uncoupled to the scattering states of the electromagnetic field at the Γ point keeping a large Q ($\geq 2\times 10^5$) for a relatively wide set of values of in-plane $k_{||} \leq 0.1(2\pi/a)$ (see Fig. 1 (b)). This high Q for a large $k_{||}$ values can be explained as follows. When $R_g/a = R_t/a \leq 1/\sqrt{3}$, the hybrid lattice becomes a triangular lattice of pitch $a/\sqrt{3}$. The triangular lattice can be calculated either with the 2D Bravais lattice of the hybrid lattice, lattice constant a (Fig. 1 a), or with its natural lattice constant ($a/\sqrt{3}$). Using the Bravais lattice of the hybrid structure (blue line in Fig. 2), the bands are folded within a Brillouin zone which area is a factor of three times smaller. The calculated photonic bands using the Bravais lattice of the triangular lattice with its natural constant $a/\sqrt{3}$ are also shown in Fig. 2 (red dots). The Γ_3 state of the hybrid lattice (see Fig. 1 (b)) corresponds to a maximum of the first band at the K_1 point of the triangular lattice (see Fig. 2), which is below the light line. The mode of the triangular lattice is non-radiative, and is rendered weakly radiative by the small perturbation consisting in the different radius between the two sets of holes of the hybrid lattice. The mechanism for the formation of these high-Q states is unrelated with the flat bands of the hybrid lattice (which are number 4 and 5), and is more similar to the mechanism of heterostructure cavities [20], where a small perturbation in the lattice yields a very high Q-factor. However, the Γ_3 state is a delocalized state (not a cavity mode) because the perturbation is periodic rather than localized. It must be noted that Q calculated is for an infinite in-plane structure where there is no in-plane losses and the Q of the structure is limited by the vertical quality factor Q_v. For finite size structures, with lateral size L, the value of the Q calculated by the gme method, i.e., for an infinite lateral size structure, must correspond to the Q_v of the finite size structure assuming $k_{||} \sim 1/L$ is very close to Γ.

3. Fabrication and Optical characterization

3.1. Fabrication

The PC consists in a InP slab with a thickness of $t = 237$ nm. It contains four InAsP quantum wells as active layer grown by molecular beam epitaxy (MBE) on an InP wafer. An InGaAs 300 nm is used as sacrificial-stop layer in the selective wet etching. The structure is transfered to the top of a Si subtrate by SiO_2 wafer bonding [21]. The thickness of the SiO_2 is 0.9 ± 0.1 μm. The InP carrier wafer is removed by wet chemical etching. A 120 nm thick SiO_2 layer is deposited by plasma enhanced chemical vapor deposition. Processing of the PC structures was done by electron beam lithography on a polymethylmethacrylate (PMMA) layer on top of the

#112644 - $15.00 USD Received 10 Jun 2009; revised 18 Jul 2009; accepted 20 Jul 2009; published 10 Aug 2009

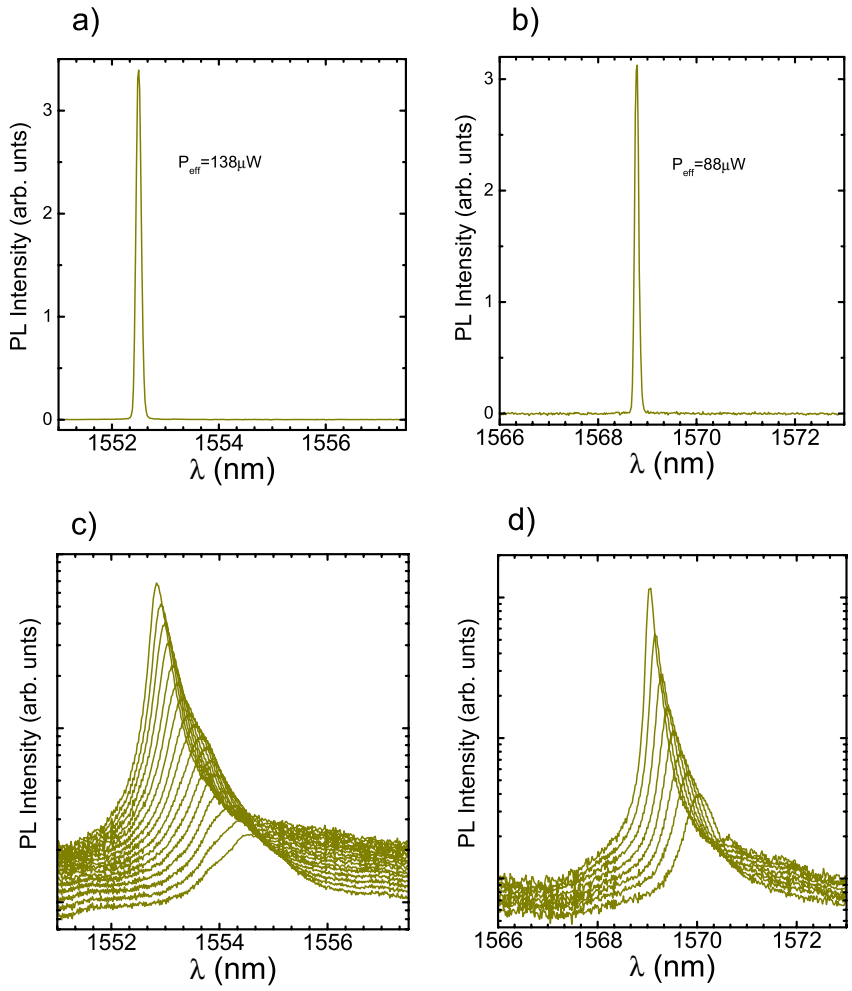

Fig. 4. Top graphs shown spectra measured above the threshold for two structures: a) Spectrum of the *A* structure. b) Spectrum of the *B* structure. Bottom graphs shows the spectra measured well below the threshold for *A*, *B* structures. c) Spectra of the structure (*A*) with a=760 nm at excitation effective power range from 36 to 108 μW. d) Spectra of the structure (*B*) a=780 nm at excitation effective power range from 36 to 68 μW.

SiO_2. Reactive ion beam etching (RIBE) was used to open the holes in the SiO_2 by a CHF_3/N_2 mixture. The hard mask pattern was transfered to the semiconductor material by reactive ion etching (RIE) by a CH_4/H_2 mixture combined with O_2 plasma cycling [22]. After the process a thick layer of SiO_2 ($\sim$ 80 nm) remains on the top of the sample. The lateral size of the fabricated structures was 30×30 μm^2. Structures with lattice parameters ranging from 760 nm to 815 nm were fabricated. We have selected two structures with a=760 and a=780 nm (Fig. 3) in order to tune the selected Bloch mode with the optimum region of the photoluminescence (PL) spectra. The values of the hole radii have been kept around $R_t/a \sim 0.12$ and $R_g/a \sim 0.17$.

#112644 - $15.00 USD Received 10 Jun 2009; revised 18 Jul 2009; accepted 20 Jul 2009; published 10 Aug 2009

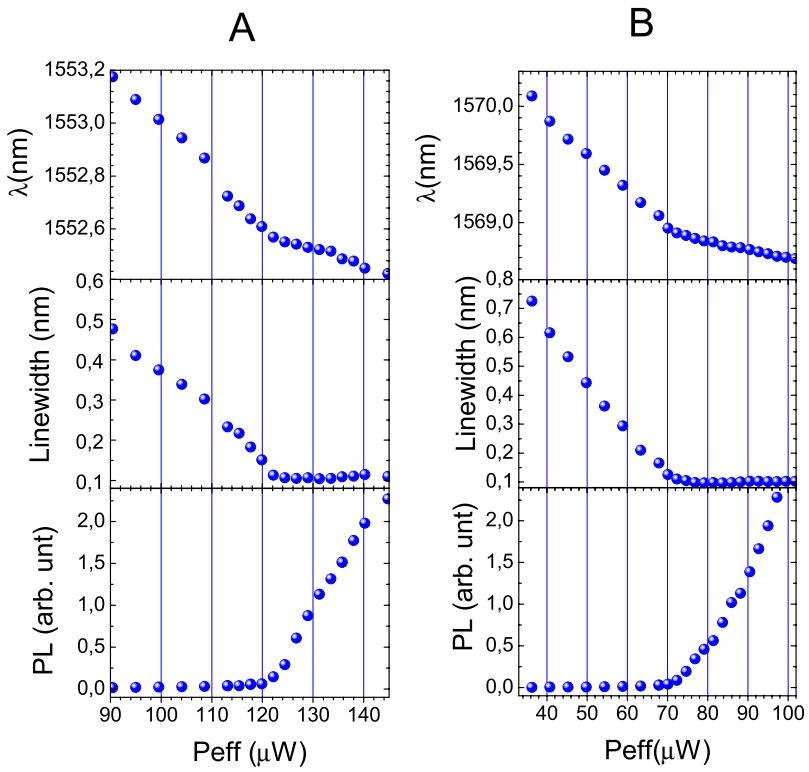

Fig. 5. Evolution with the excitation effective power. Left: Structure *A*. Right: Structure *B*.

3.2. Optical characterization

The optical characterization was performed by microphotoluminescence (μ-PL) spectroscopy at room temperature. The structures were optically pumped with a 785 nm laser diode to a frequency of 1 MHz and a 2.5% duty cycle. An objective lens $(0.14\ NA)$ is used to focus the excitation spot (diameter is $\sim 10\ \mu$m). The emitted light is collected through an optical fiber connected to an optical spectra analyzer or dispersed by a 0.85 m focal length double spectrometer with a cooled InGaAs photodiode array as detector.

Laser emission from 1.55 μm to 1.57 μm have been obtained for different fabricated structures, with effective pump power threshold around 70 μW, and Qs between 10000-12000. The absorbed pump power was obtained by the method described in Ref. [23]. The reflectivity of the InP was estimated to be $\sim 30\%$, and the absorption coefficient $\alpha = 12900 cm^{-1}$ [24] giving an absorption fraction of $\sim 24\%$. Fig. 4 shows spectra for two of the structures, *A* with *a*= 760 nm and *B* with *a*=780 nm, below and above of the excitation pump power threshold. The spectra of both structures have a lorentzian lineshape more clearly at high excitation powers. At low excitation powers the PL background added with the Bloch mode emission give a not lorentzian shape of the peak. A decrease of the linewidth and a blueshift are observed as the excitation power is increased. The emission wavelength of the peak is in good agrement with the calculated ones (Fig. 1 (b)).

#112644 - $15.00 USD Received 10 Jun 2009; revised 18 Jul 2009; accepted 20 Jul 2009; published 10 Aug 2009

Figure 5 shows the emission wavelength of the laser peak, the measured linewidth, and the integrated emission intensity versus the effective pump power for both structures. A clear non linear emission is observed with an effective pump power threshold $P_{th} = 120\ \mu$W and with a $Q = 10000$ just below the threshold for the structure *A*. Taking into account the excitation spot size, we obtained a threshold density of power excitation of $\sim$150 W/cm^2. Similar behavior is observed for the second structure with $P_{th} = 70\ \mu$W, $Q = 12000$, and a threshold density of power excitation $\sim$100 W/cm^2. It is important to note that we approximate the Q of the cold cavity for the value $\lambda/\Delta\lambda$ just below the lasing threshold [25]. This does not make sure that we are exactly at the transparency pump power. The Q measured bellow the threshold is similar for all the structures studied and is close to previously Γ-point 2D-PC lasers [11, 12] operating a 1.55 μm without bottom Bragg reflector. Nevertheless, the threshold value is around three times higher (in term of incident peak power at threshold) than the reported in Ref. [12] on InAsP/InP substrates bonded to SiO_2. In that case, however, the pumping conditions are different.

The lasing linewidth well above the threshold is limited by the linewidth enhancement factor (α). The linewidth measured is not limited by the spectral resolution of our experimental set-up. For the sample *A* the linewidth saturates before than sample B (see Fig. 5). This means that $\alpha_A > \alpha_B$. Since the differential refractive index is mainly a material parameter, the variation of α from structure to structure has its source in the variation of differential gain [26]. By other hand, α is inversely proportional to the emission wavelength and to the variation of the optical gain with the number of carriers (dg/dN). Then, we conclude that $(dg/dN)_B > (dg/dN)_A$. This means that the emission of sample *B* is in a better spectral position than for *A*, which implies the reduction in the power threshold, which is due to the best relation absorbtion-gain for the spectral position of the Bloch mode of the *B* structure and its higher Q [27]. The evolution of the peak position with the excitation power presented for both structures a linear behavior with two different stages. Below the threshold the blueshift is faster than above the threshold as it is expected for lasers with good heat dissipation [28]. This is the common case for the structures wafer bonded to a Si substrate [29]. The blueshift above the threshold is due to the carrier induced modification of the refractive index [30, 31]. We have shown in previous publications [30, 31], that free-carrier optical generation can significantly blue-shift the emission wavelength. Beyond threshold, free carrier density is clamped (at least partially [31]), which results in the observed saturation of the blue shift.

It must be noted that the value of the Q measured is slightly higher than the estimated for the finite size structure (lower than $\sim$ 8000). This can be explained by the finite size of the mode and the reduction of the lateral leakage. The size of the mode can be controlled by the pump beam area through the carrier generation that induces (Kerr effect) a blue shift of the resonance [30]. This effect results in a localization of the slow Bloch mode around a high symmetry extreme of the dispersion characteristics with negative curvature. The lateral extension of the Bloch mode is therefore limited to the pumping area [6]. The lateral leakage is due to the finite size of the structure and the matching of its modes with the waveguide modes [10]. In our case the above mentioned effects are not enough to explain the important increase of the Q compared to the estimated. We attribute this increase to the effect of a small variation of the radii of the holes close to the borders of the structure. As it has been demonstrated recently [32, 33, 34] a slight variation in the size of the features close to the borders strongly reduces the in-plane lateral leakage.

In Γ-point PC structures with finite size there are two mechanisms of the Q limitation. The first one is the lateral escape of the photons at the borders of the structures. The second is due to the finite size of the mode that contains photons with $k_{||} \neq 0$, then vertical losses around the Γ point appear and can be significant. In the hybrid triangular-graphite lattice the Bloch mode selected presents a high Q_v for a wide range of $k_{||}$ in-plane vectors around the Γ point

#112644 - $15.00 USD Received 10 Jun 2009; revised 18 Jul 2009; accepted 20 Jul 2009; published 10 Aug 2009

that reduces the vertical losses due to the finite size of the mode. This may allow the design of a Γ_3 point heterostructure [20] for suppressing the lateral leakage with smaller lateral size and strongly higher Q [32]. Moreover, the intensity of emission could be enhanced by combining the structure with a bottom Bragg reflector [19].

4. Summary

We have demonstrated room temperature surface emitting PC laser operating around 1.55 μm using the PC structure of the hybrid triangular-graphite lattice. By optical pumping the structure presents a low threshold of excitation power ($\sim$70-120 μW). Quality factors ranging from 10000 to 12000 have been measured.

The Bloch mode (Γ_3 point) selected for the vertical emission presents a high quality factor for a wide range of $k_{||}$ in plane vectors around the Γ point. This high Q is explained by the correspondence of this mode above the light line with the first *K* point of the triangular lattice below the light line which is rendered weakly radiative due to the perturbation induced by the two sets of holes of the hybrid lattice. This allows the design of a Γ_3 point heterostructure to inhibit the lateral leakage of the photons giving place a PC structure with strongly high Q, relative small modal volume, and vertical directional emission.

Acknowledgments

L.J. Martínez thanks an I3P fellowship and I. Prieto thanks a FPI fellowship BES-2006-13649. The authors would like to acknowledge support from CONSOLIDER-Ingenio (CSO2006-00019 (QOIT)) 2010, CAM Nanocomic (S-0505ESP0200), Naninpho-QD (TEC2008-03756-C03-01)) and Fondazione CARIPLO. The epitaxial structure was grown by Philippe Regreny, at INL. J.M. Fedeli and L. Di Cioccio, from CEA-LETI, are acknowledged for the wafer bonding.

#112644 - $15.00 USD Received 10 Jun 2009; revised 18 Jul 2009; accepted 20 Jul 2009; published 10 Aug 2009